Supplementary Information:

Anion and Cation Effects on Size Control of Au Nanoparticles Prepared by Sputter Deposition in Imidazolium-based Ionic Liquids

Yoshikiyo Hatakeyama,[a] Ken Judai,[a] Kei Onishi,[b]
Satoshi Takahashi,[b] Satoshi Kimura,[b] and Keiko Nishikawa[b]

[a]*College of Humanities and Sciences, Nihon University, Sakurajosui, Setagaya-ku, Tokyo 156-8550, Japan*
[b]*Graduate School of Advanced Integration Science, Chiba University, Yayoi-cho, Inage-ku, Chiba 263-8522, Japan*

TEM Images (Fig. S1)

TEM images of AuNPs prepared in [C_4mim]BF_4 at 60 °C and in [C_4mim][TFSA] at 30 °C are shown in Fig. S1 as typical examples. Although the shapes of AuNPs are basically spherical in both the solutions, an apparent size difference is observed. Namely, while the AuNPs generated in [C_4mim]BF_4 are 2.4–4.0 nm in size, those in [C_4mim][TFSA] are much larger (4.3–8.6 nm) and the size distribution is more scattered. These values are larger than the ones determined by SAXS analyses (see Figs. S6 (a) and S6 (d)). We think this is because of the growing and aggregation during the preparative operation for TEM experiments.[S1] In this connection, it is reported that the sizes of spherical AuNPs determined by TEM and SAXS observations are almost the same, when the spherical AuNPs are strongly bonded with the stabilizing agents such as thiols and as a result the AuNPs have little possibility to grow by gathering.[S2]

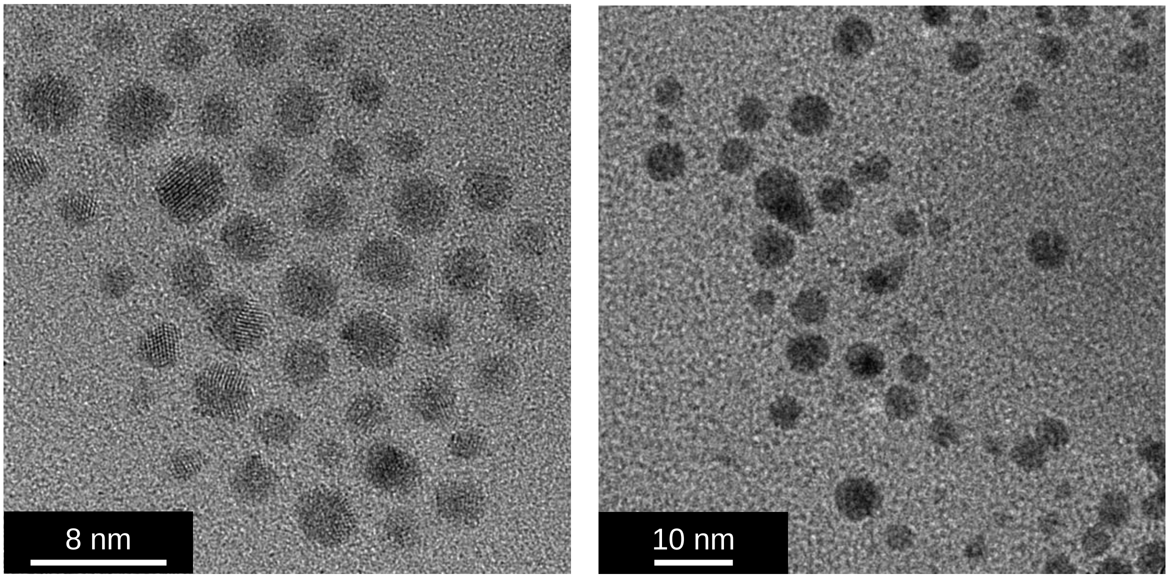

Fig. S1. TEM images of AuNPs generated in [C_4mim]BF_4 at 60 °C (left) and (b) [C_4mim][TFSA] at 30 °C (right).

UV–Vis Spectra (Fig. S2–S4)

Figs. S2–S4 show the temperature dependences of absorption spectra around the surface plasmon resonance (SPR) bands of AuNPs prepared in the ionic liquids. Comparing these results, remarkable differences in the spectra are observed. First, only in the spectra of AuNPs prepared in ILs with BF_4 anions (Fig. S2), we observe the noticeable SPR absorption band around 520 nm as a peak or shoulder and the intensity increases as rise of the preparation temperature, namely increase of the size of NPs. In contrast, other spectra have little or no plasmon bands. It is well known that the peak position and absorbance of the SPR band depend on AuNPs' size and shape.[S3] Namely, in the case of spherical AuNPs less than 2 nm in size, the plasmon band disappears.[S4,S5] In addition, the absorbance of SPR is reported to decrease due to the surface binding with stabilizing agents having thiol groups.[S6,S7] In the present cases, both the two factors, size and coordination of ILs, are necessary to be considered. For BF_4^- series, the size effect conspicuously seems to work. On the other hand, for IL with [OTf], [FSA] and [TFSA] anions, it is thought that the SPR bands are affected by strong interactions with the anions. So, SPR bands are not observed even for larger AuNPs generated in the ILs with [OTf], [FSA] and [TFSA] anions.

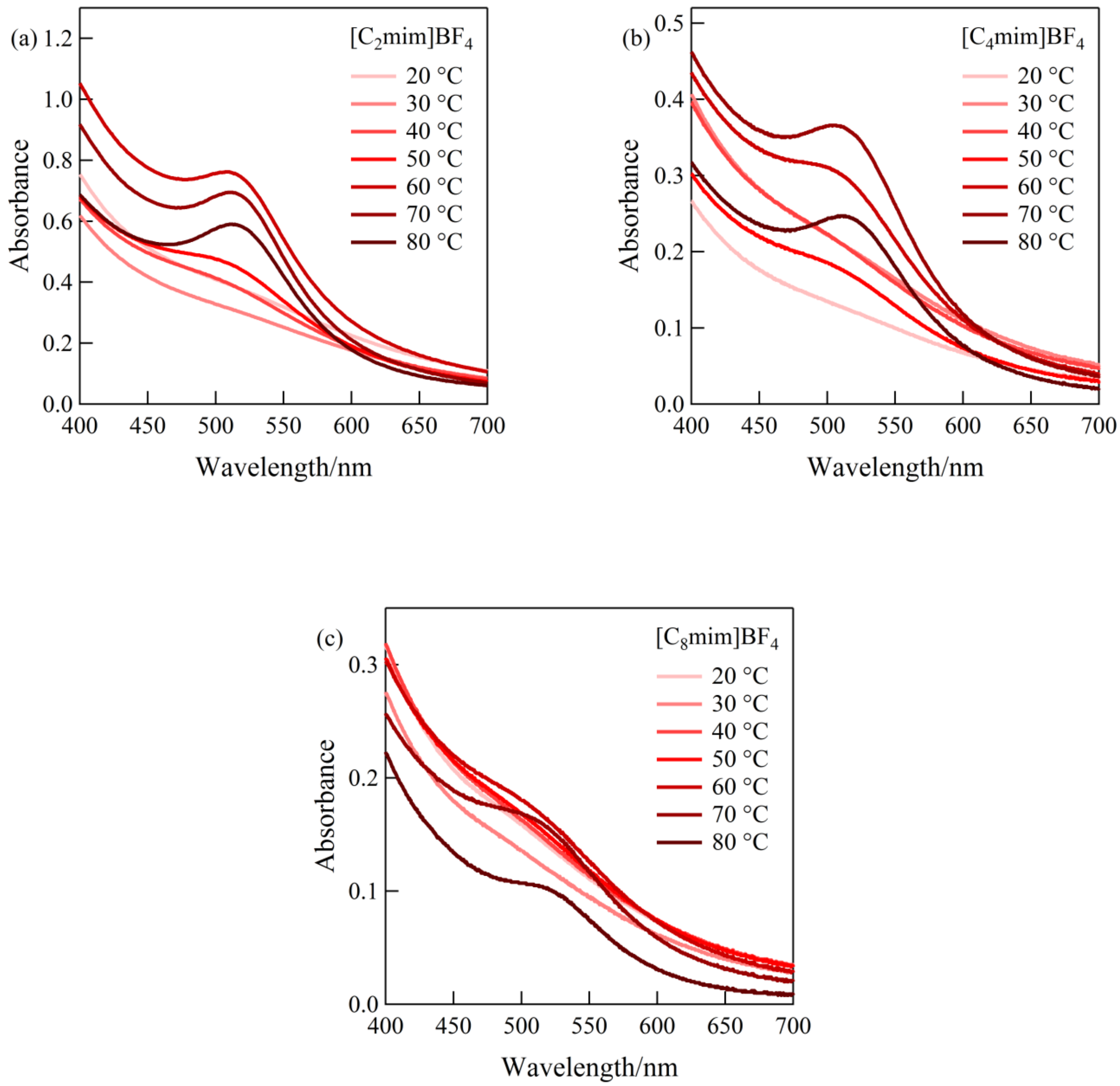

Fig. S2. UV–Vis absorption spectra of AuNPs around plasmon band generated in (a) $[C_2mim]BF_4$, (b) $[C_4mim]BF_4$, and (c) $[C_8mim]BF_4$ at different temperatures.

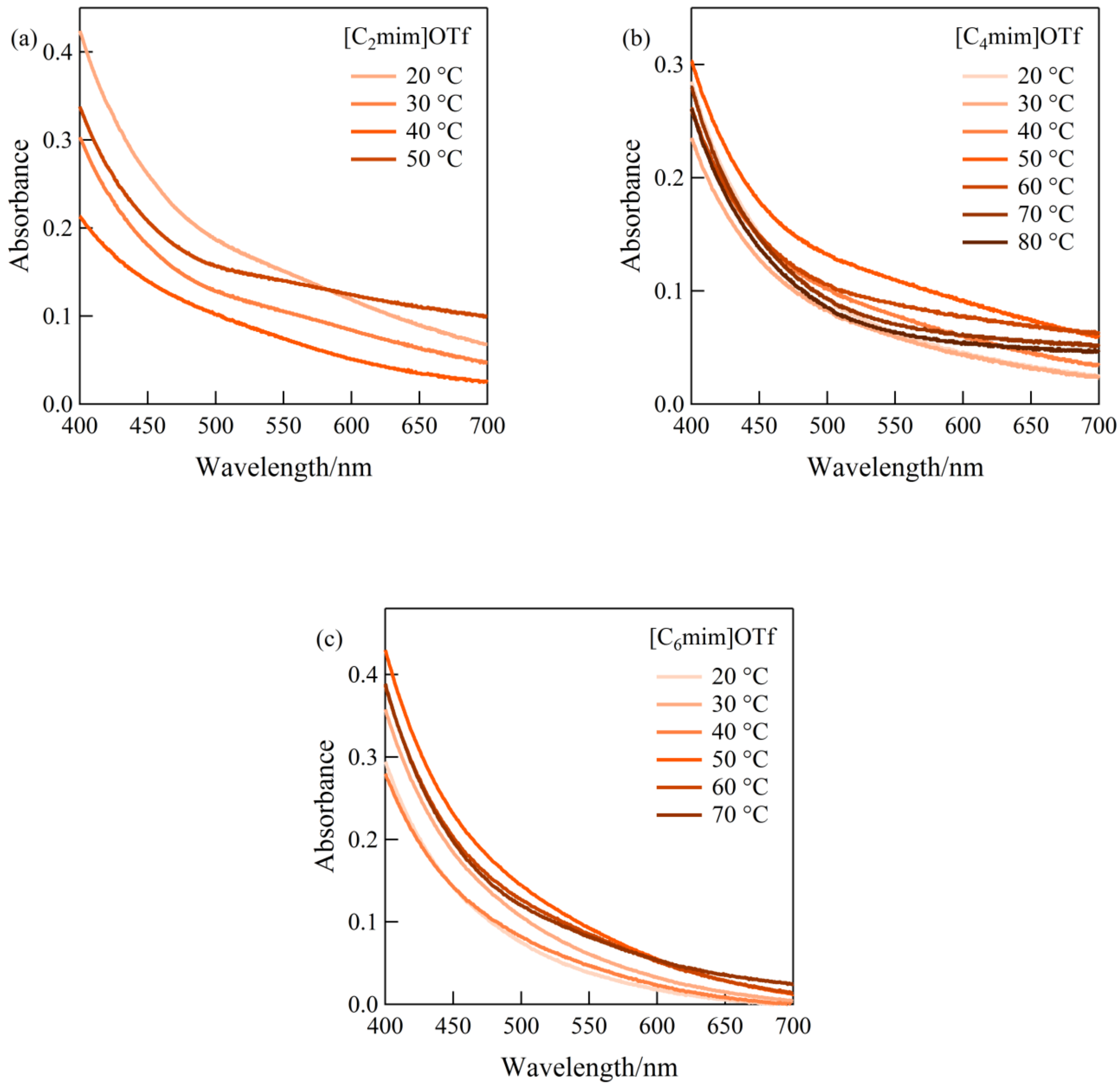

Fig. S3. UV–Vis absorption spectra of AuNPs around plasmon band generated in (a) [C_2mim]OTf, (b) [C_4mim]OTf, and (c) [C_6mim]OTf at different temperatures.

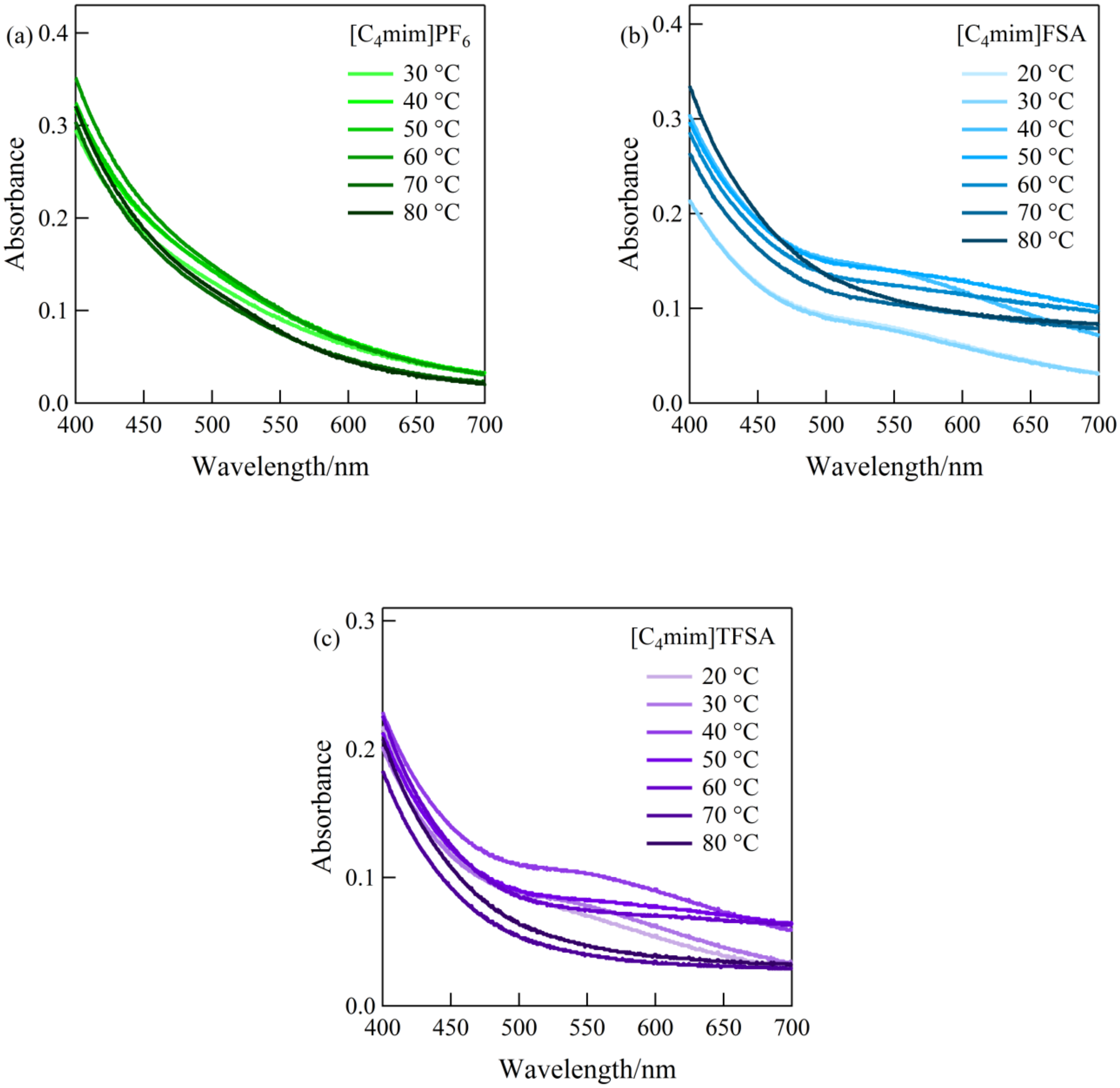

Fig. S4. UV–Vis absorption spectra of AuNPs generated in (a) [C_4mim]PF_6, (b) [C_4mim][FSA], and (c) [C_4mim][TFSA] at different temperatures.

SAXS profiles and particle size distribution functions. (Figs. S5–S8)

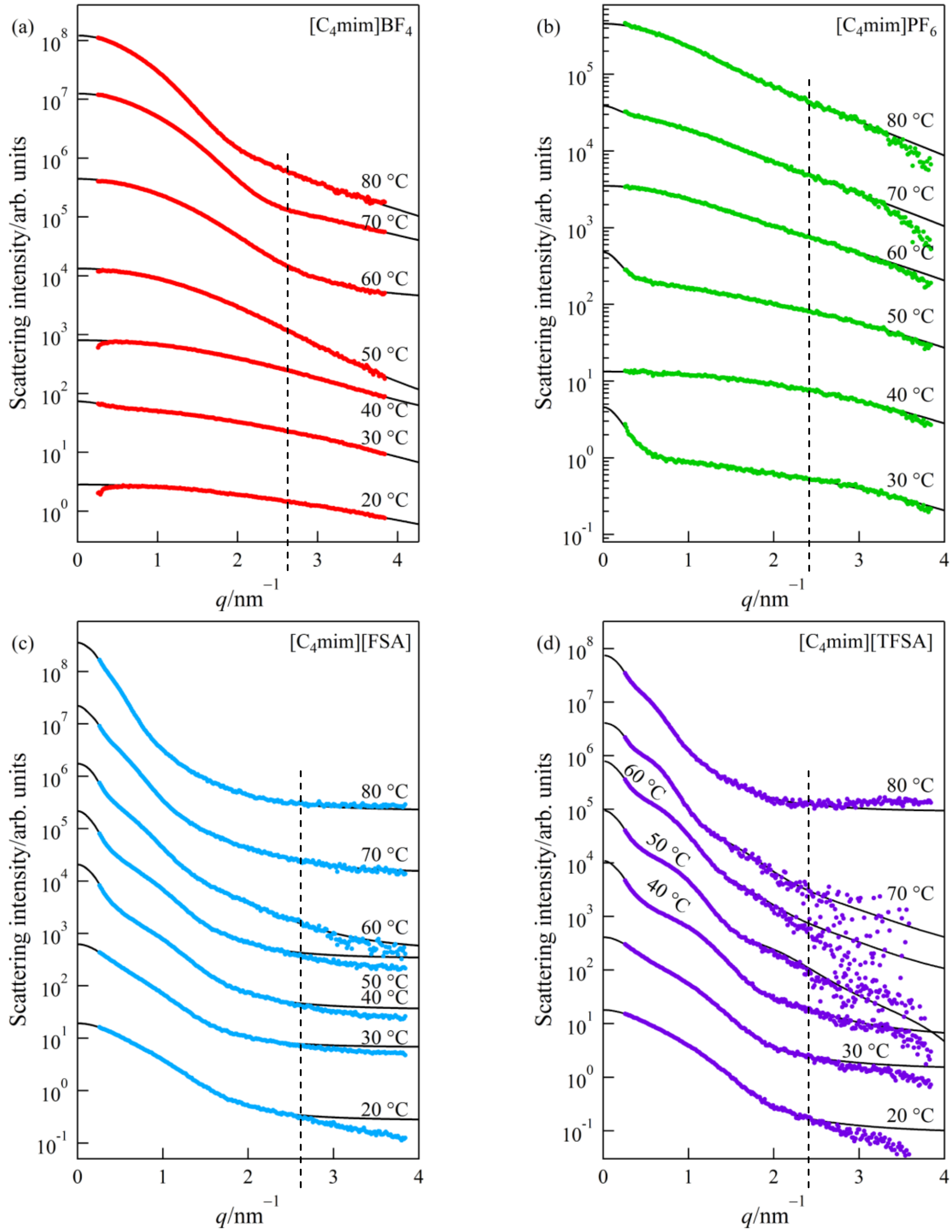

Fig. S5. SAXS profiles of AuNPs generated in (a) [C_4mim]BF_4, (b) [C_4mim]PF_6, (c) [C_4mim][FSA], and (d) [C_4mim][TFSA] at different temperatures. For the fitting analysis, we used data from the smaller *q*-region to the left of the dashed lines.

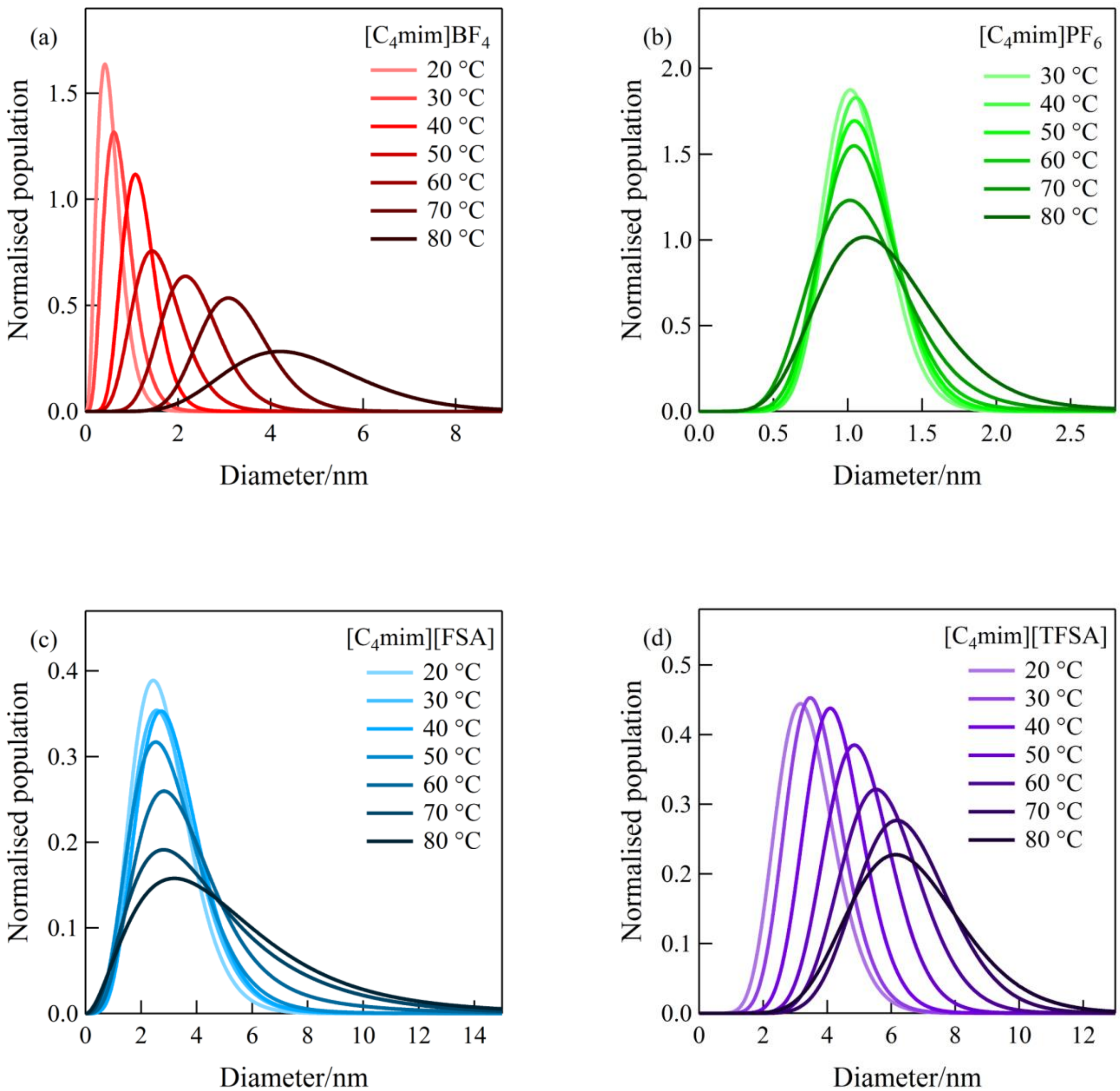

Fig. S6. Particle size distributions of AuNPs generated in (a) [C_4mim]BF_4, (b) [C_4mim]PF_6, (c) [C_4mim][FSA], and (d) [C_4mim][TFSA] at different temperatures.

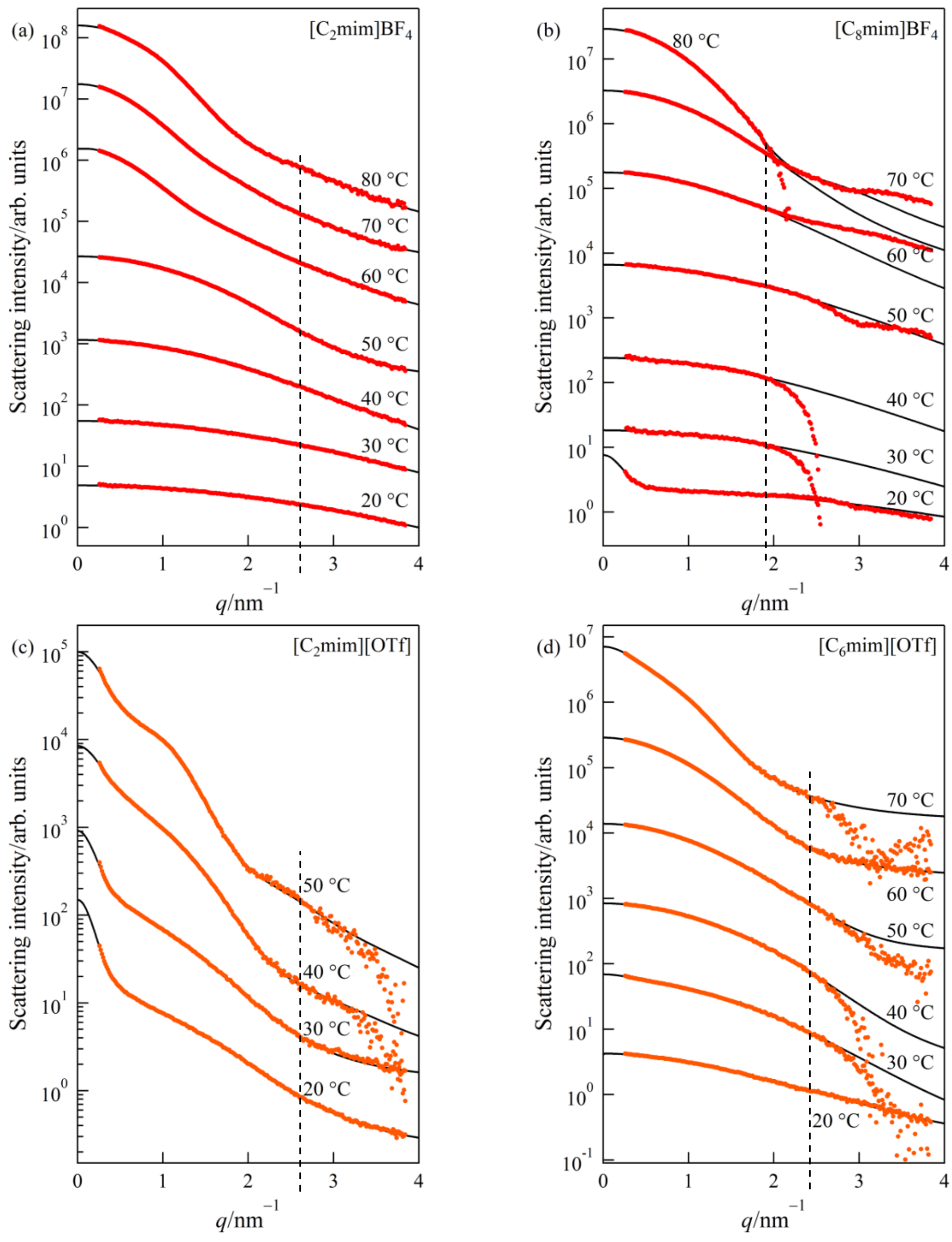

Fig. S7. SAXS profiles of AuNPs generated in (a) $[C_2mim]BF_4$, (b) $[C_8mim]BF_4$, (c) $[C_2mim][OTf]$, and (d) $[C_6mim][OTf]$ at different temperatures. For the fitting analysis, we used data from the smaller q-region to the left of the dashed lines.

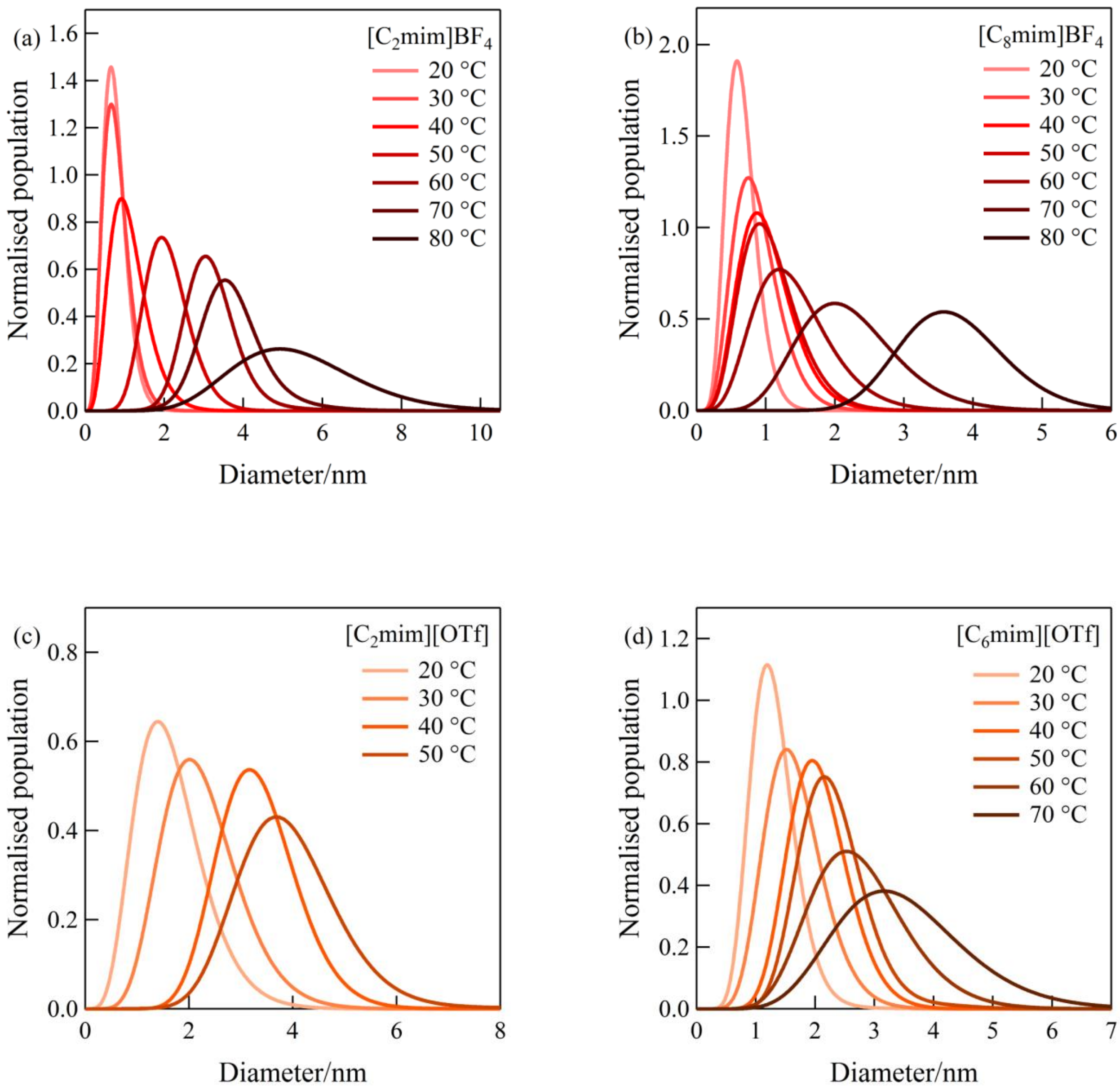

Fig. S8. Particle size distributions of AuNPs generated in (a) [C_2mim]BF_4, (b) [C_8mim]BF_4, (c) [C_2mim][OTf], and (d) [C_6mim][OTf] at different temperatures.

Temperature dependences of the densities of the used ionic liquids (Fig. S9)

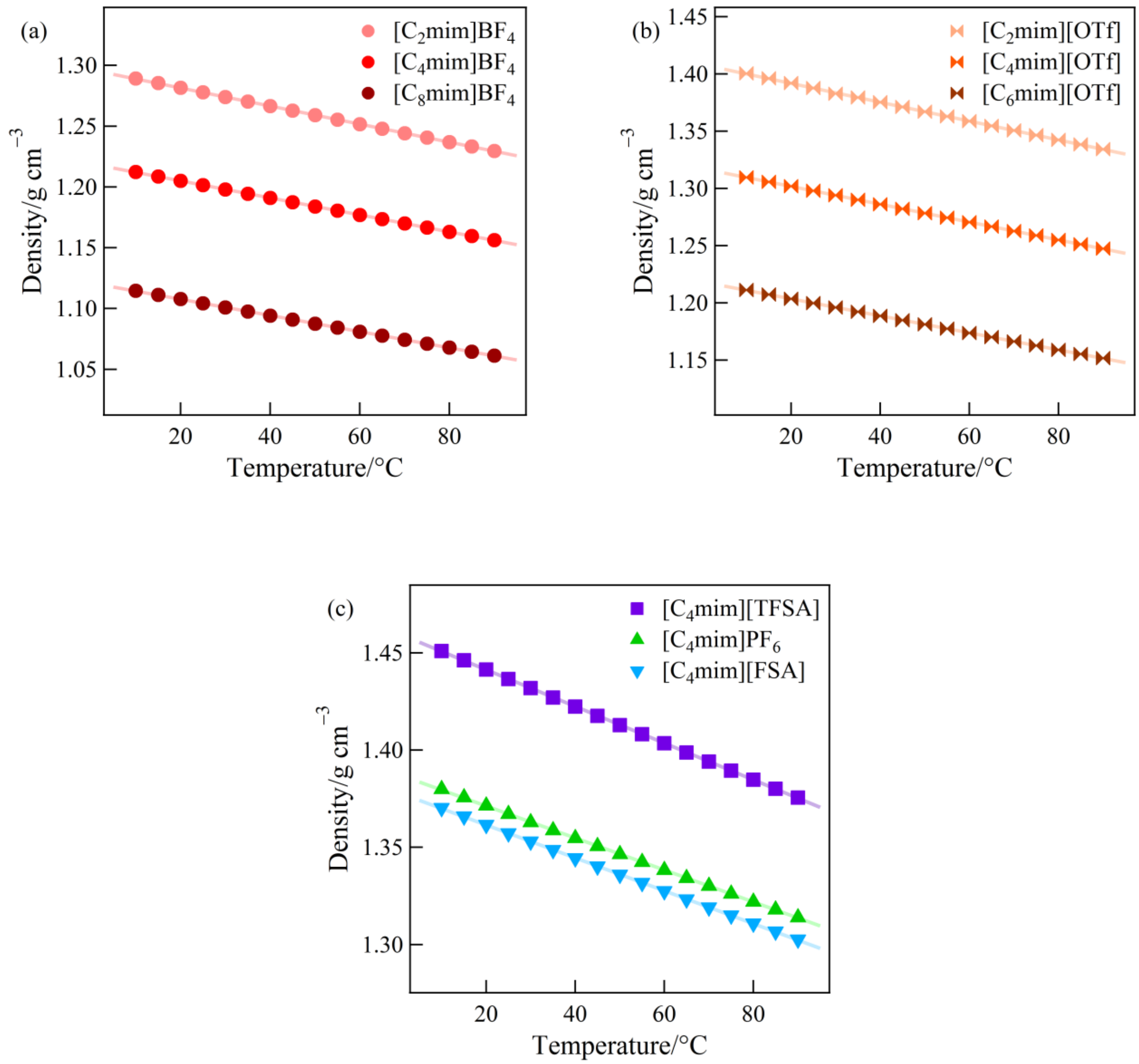

Fig. S9. Temperature dependences of the densities of the ionic liquids used to prepare the AuNPs. (a) $[C_2mim]BF_4$, $[C_4mim]BF_4$, and $[C_8mim]BF_4$. (b) $[C_2mim][OTf]$, $[C_4mim][OTf]$, and $[C_6mim][OTf]$. (c) $[C_4mim]PF_6$, $[C_4mim][FSA]$, and $[C_4mim][TFSA]$.

Temperature dependences of the viscosities of the used ionic liquids (Fig. S10)

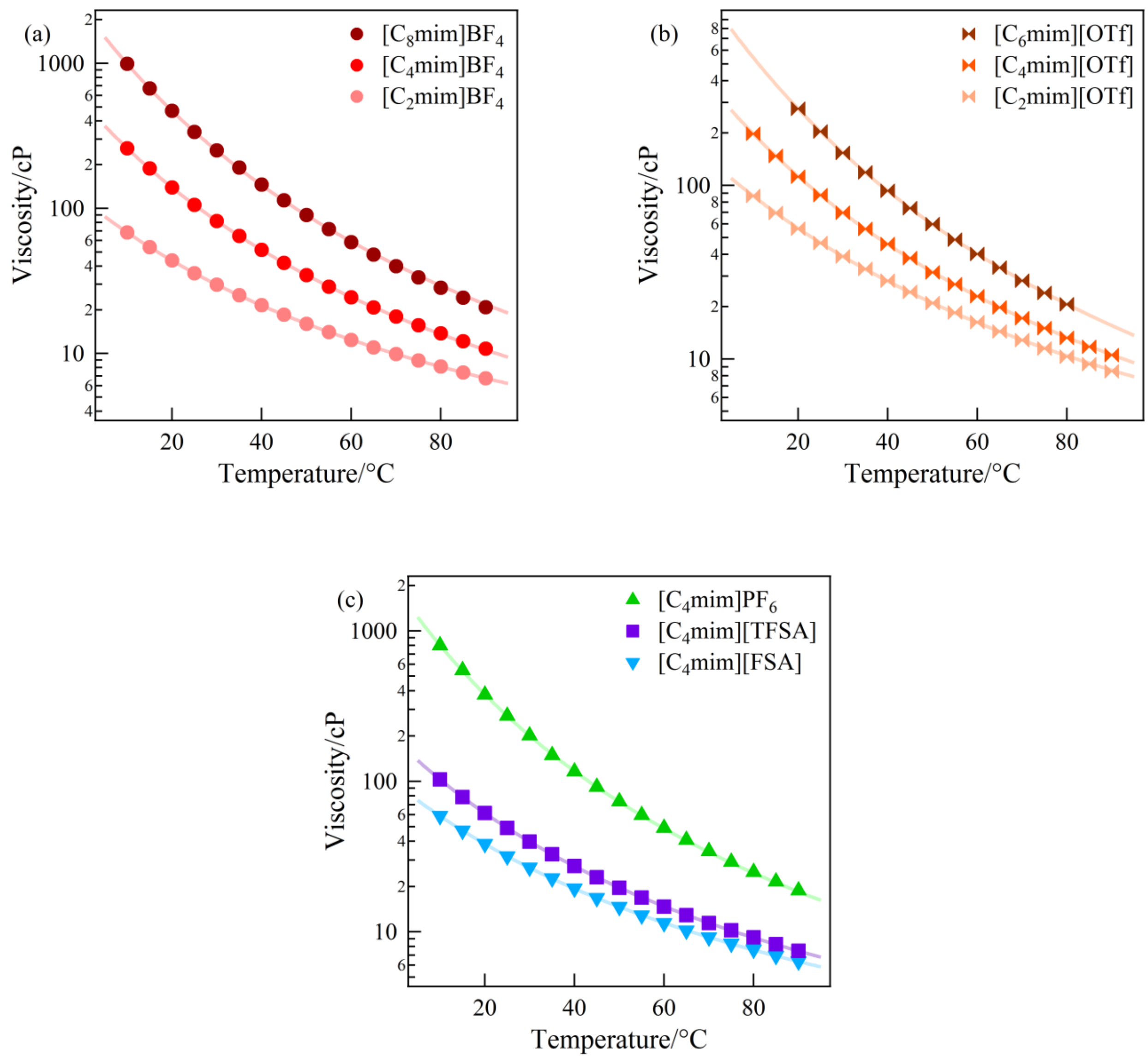

Fig. S10. Temperature dependences of the viscosities of the ionic liquids used to prepare the AuNPs. The solid lines correspond to the fit of the data by the Vogel–Tamman–Fulcher (VTF) equation. (a) [C_2mim]BF_4, [C_4mim]BF_4, and [C_8mim]BF_4. (b) [C_2mim][OTf], [C_4mim][OTf], and [C_6mim][OTf]. (c) [C_4mim]PF_6, [C_4mim][FSA], and [C_4mim][TFSA].

References

S1. Y. Hatakeyama, T. Morita, S. Takahashi, K. Onishi and K. Nishikawa, *J. Phys. Chem. C*, 2011, **115**, 3279–3285.

S2. H. Koerner, R. I. MacCuspie, K. Park and R. A. Vaia, *Chem. Mater.*, 2012, **24**, 981–995.

S3. S. Link and M. A. El-Sayed, *J. Phys. Chem. B*, 1999, **103**, 4212–4217.

S4. Y. Negishi and T. Tsukuda, *J. Am. Chem. Soc.*, 2003, **125**, 4046–4047.

S5. G. H. Woehrle, M. G. Warner and J. E. Hutchison, *J. Phys. Chem. B*, 2002, **106**, 9979–9981.

S6. G. C. Lica, B. S. Zelakiewicz, M. Constantinescu and Tong, *J. Phys. Chem. B,* 2004, **108**, 19896–19900.

S7. Y. Hatakeyama, J. Kato, T. Mukai, K. Judai and K. Nishikawa, *Bull. Chem. Soc. Jpn.*, 2014, **87**, 773–779.